Institute of
Ionosphere

On solar sources of interplanetary disturbances before the high-energy magnetospheric electrons enhancements

O.N. Kryakunova[1], A.V. Belov[2], B.B. Seifullina[1], A.A. Abunin[2], M.A. Abunina[2], I.L. Tsepakina[1], N.F. Nikolayevskiy[1], N.S. Shlyk[2], R.E. Koichubayev

(krolganik@yandex.ru)

[1] Institute of the Ionosphere, Almaty, Kazakhstan

[2] Pushkov Institute of Terrestrial Magnetism, Ionosphere and Radio Wave Propagation (IZMIRAN), Russian Academy of Sciences, Troitsk, Moscow, Russia

First Workshop on Sun and Space Weather
Antalya, Türkiye

1. Introduction



The study of relativistic magnetospheric electrons with energies >2 MeV is one of the most important tasks of magnetospheric physics and space weather.

The dynamics of the electron flux behavior is very complex; it can change by some orders of magnitude over several days, depending on the state of the interplanetary and near-Earth environment. Sharp increases and decreases in the electron flux can be attributed to extreme space weather events.

The day-to-day variability of the high-energy electron flux is related to conditions in interplanetary and near-Earth space. Increases in high-energy magnetospheric electron fluxes occur after the arrival of interplanetary disturbances to the Earth with a delay of 1-2 days.

Project INTAS-00-0810 **"Improvement of methods of control and prognosis of periods of dangerous influence of space weather on satellite's electronics"**

high alt.- low incl.

cc=0.40

- **e>2 MeV**
- Apd, AEd, sf
- Vsw
- p60d, p100
- da10

low alt.-high incl.

cc=0.21

- **e>2 MeV**
- CRA
- Apd, sf
- Vsw_{max}
- Bzd

high alt.-high incl.

cc=0.51

- **p>100 MeV, p60d**
- Bznsum

The parameters used to simulate anomaly frequencies for different orbits are listed here. Green, blue and red group. Main role is for electrons in green and blue group, especially – green. In red group protons are much more important than other indices.

Belov A., Dorman L., Iucci N., Kryakunova O., Ptitsyna N. The relation of high- and low-orbit satellite anomalies to different geophysical parameters.// in "Effects of Space Weather on Technology Infrastructure. NATO Science Series II, 2004, V.176, p. 147.

Materials & Methods

To study the behavior of the high-energy electron flux and interplanetary disturbances that caused its changes, various characteristics of the interplanetary and near-Earth environment were used for the period 1995-2025. For this work, it is assumed that the enhancement begins when the daily electron fluence exceeds 10^8 particles·cm^{-2}·sr^{-1}·day^{-1}. For the period 1995-2025, 478 such events were identified.

For all events, we carefully analyzed the state of the interplanetary and near-Earth space several days before and during high-energy electron flux enhancements, as well as solar sources of interplanetary disturbances that led to electron flux increases. It should be noted that determining solar sources of interplanetary disturbances is a rather complex task.

Data used

https://services.swpc.noaa.gov/json/goes/ (the fluxes of high-energy magnetospheric electrons with energies >2 MeV, measured on the GOES)
https://omniweb.gsfc.nasa.gov/ (SW and IMF), ftp://ftp.gfz-potsdam.de/pub/home/obs/kp-ap/wdc (Kp, Ap indices), FEID (*Forbush Effects and Interplanetary Disturbances*, https://tools.izmiran.ru/feid), https://soho.nascom.nasa.gov/, https://cdaw.gsfc.nasa.gov/CME_list/, https://ssa.esac.esa.int/ssa/#/pages/home, https://sdo.gsfc.nasa.gov/assets/img/dailymov/, https://solen.info/solar/index.html, https://solen.info/solar/coronal_holes.html), https://www.sidc.be/SILSO/datafiles

AVERAGE BEHAVIOR OF SOLAR WIND VELOCITY AND GEOMAGNETIC ACTIVITY Ap-INDEX BEFORE AND DURING ELECTRON ENHANCEMENTS IN 1987-2021

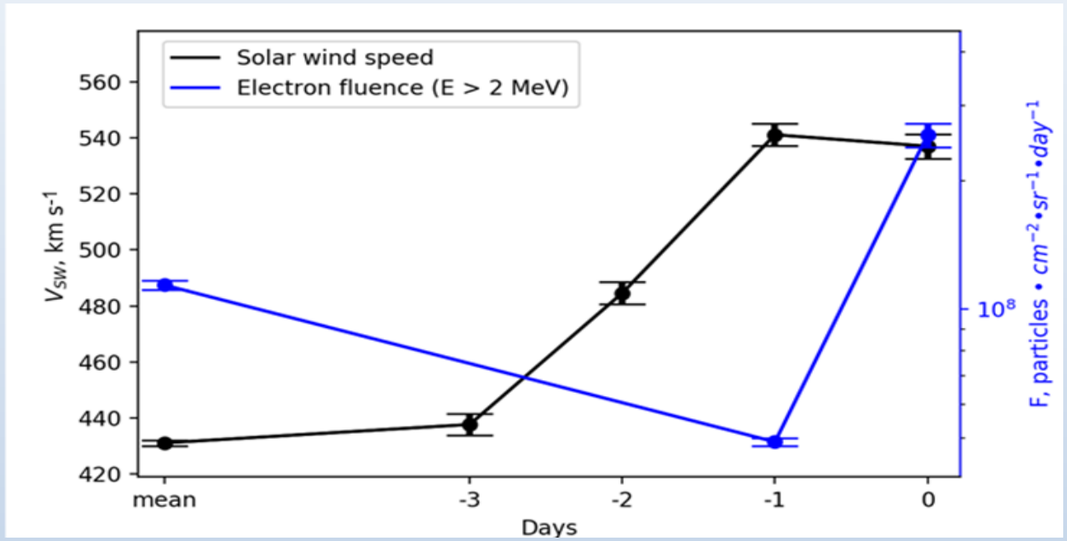

Behavior of the averaged SW velocity and diurnal fluence of magnetospheric electrons before the beginning of electron flux enhancements

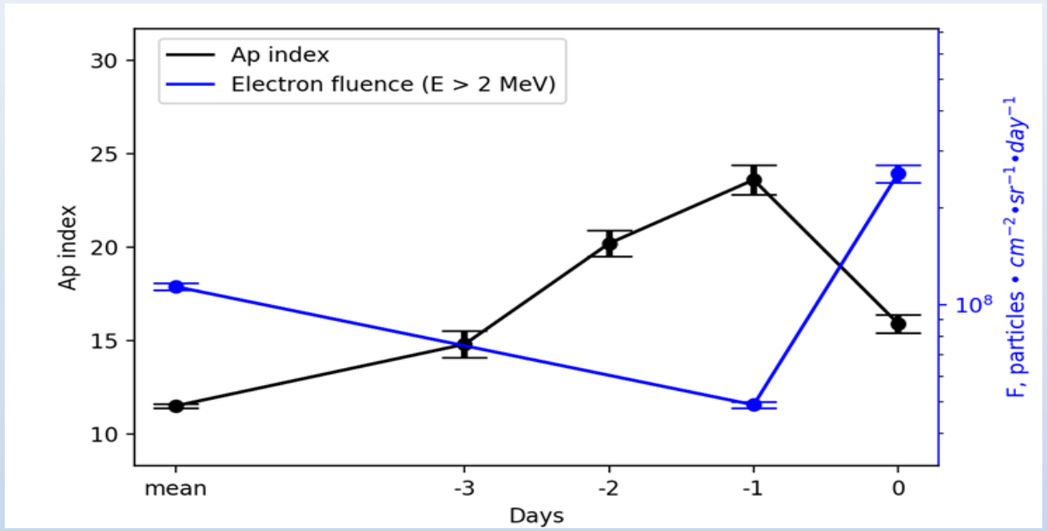

Behavior of the averaged Ap-index of geomagnetic activity and diurnal fluence of magnetospheric electrons before the beginning of electron flux enhancements

It can be seen that the SW velocity becomes elevated from Day -2, and on Day -1 it reaches the maximum, which then lasts for 2 days, covering the Day 0 as well.

On average, the Ap-index begins to grow 2 days earlier than an electron fluence enhancement occurs, and on Day -1 it reaches a level 2 times higher than the average vales for these years. One can say that the electron flux enhancement begins at the decline of geomagnetic activity after its prior increase.

Kryakunova et al. Average characteristics of high-energy magnetospheric electron flux enhancements and the parameters of near-Earth and interplanetary medium in 1987-2021. Monthly Notices of the Royal Astronomical Society, 2022.

A typical example of an event of the high-energy electron flux enhancement after the arrival of an HSS from CH

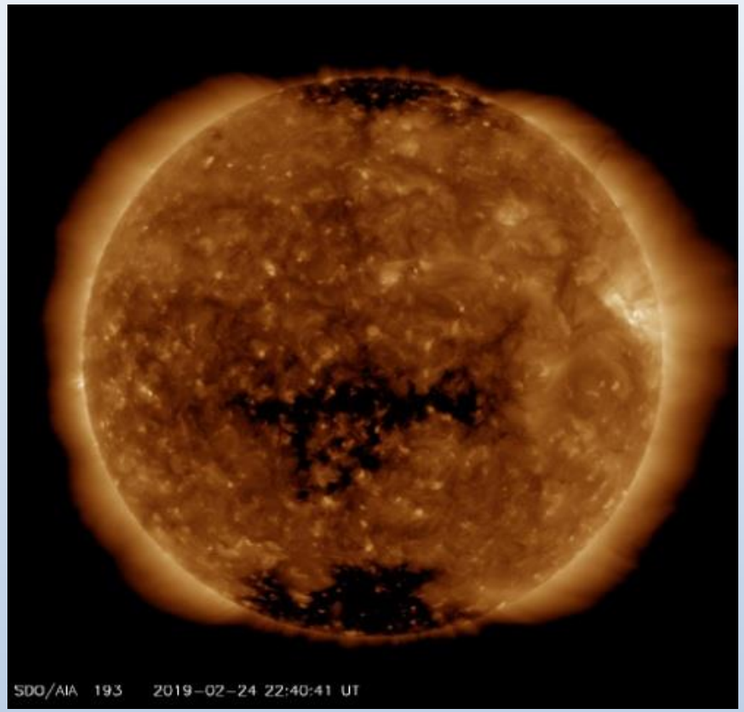

a) Solar disc image (SDO/AIA 193 data) on 2019 February 24

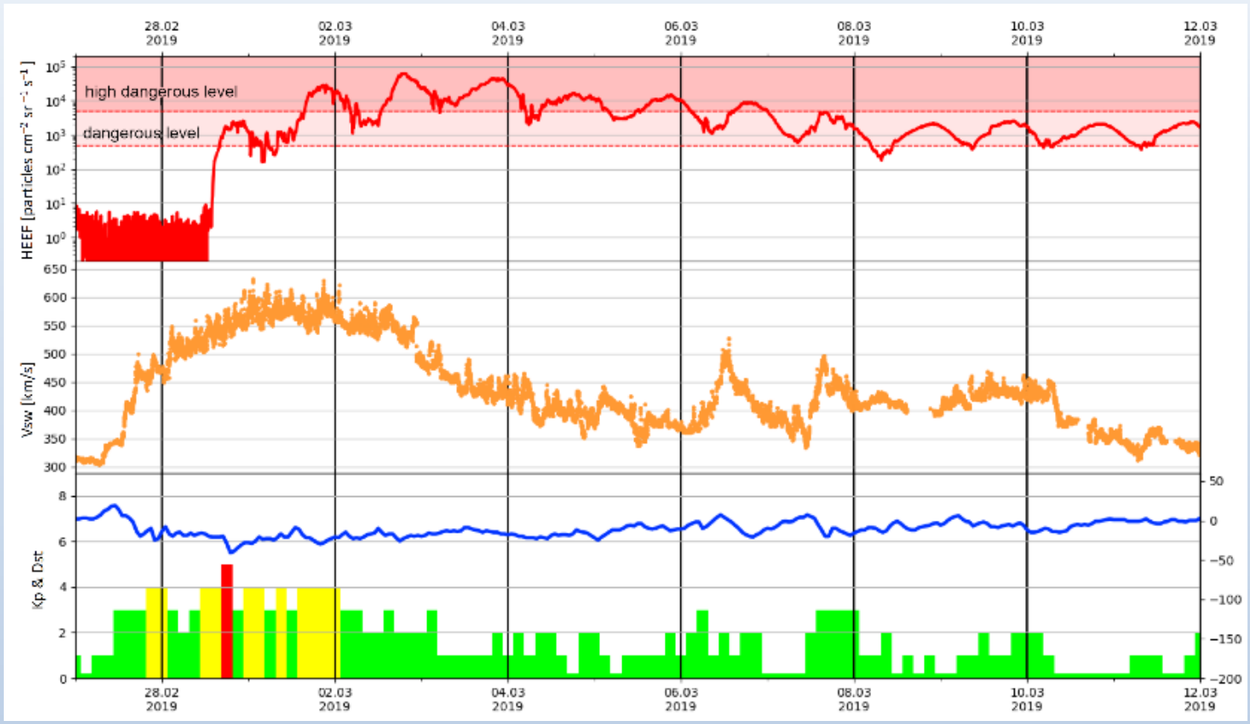

b) High-energy electron flux (upper panel), SW velocity (middle panel), and geomagnetic indices Kp and Dst (lower panel) on 2019 February 27 – March 11

This event shows a smooth increase in the SW speed typical for HSSs from CHs and an increase in geomagnetic activity from an unsettled to a minor magnetic storm level. After such a disturbance of the interplanetary and near-Earth space, the flux of high-energy electrons exceeded the super-dangerous level for 6 next days.

A typical example of an event of the high-energy electron flux enhancement after the arrival of a CME after SF

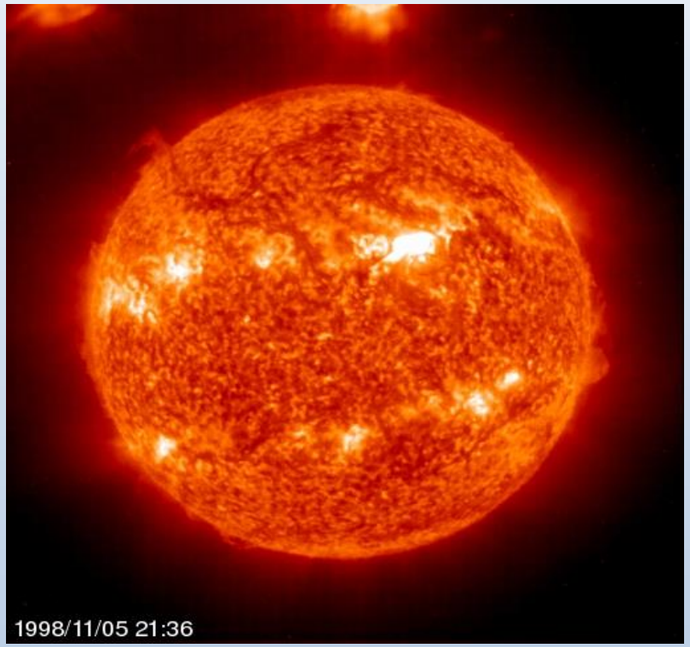

a) Solar disc image (SOHO/EIT 304 data) on 1998 November 5

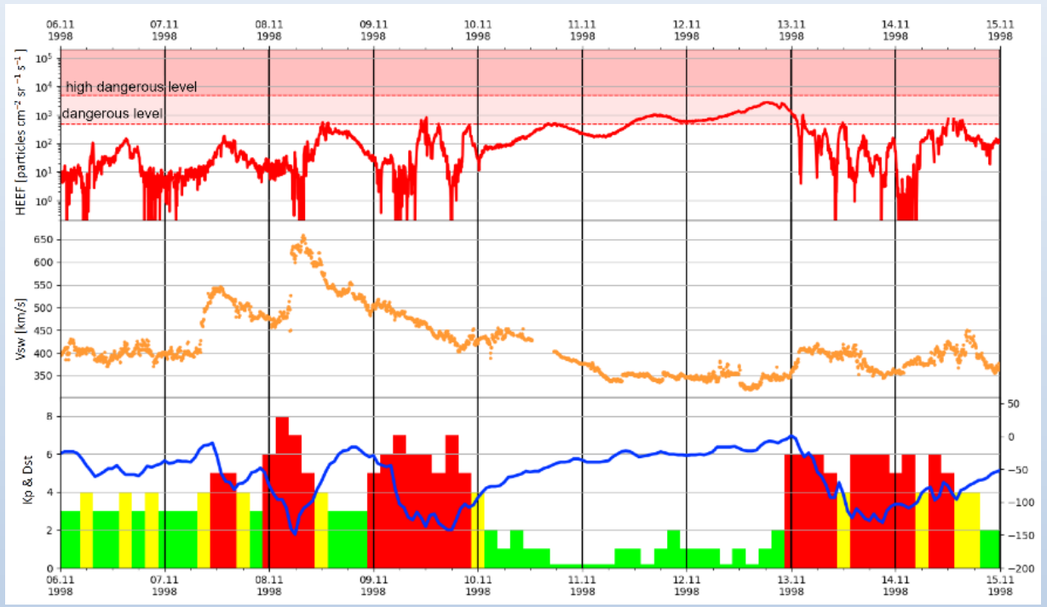

b) High-energy electron flux (upper panel), SW velocity (middle panel), and geomagnetic indices Kp and Dst (lower panel) on 1998 November 6 – 14.

In the event shown in Figures, a severe magnetic storm was observed (Kpmax=8). the geomagnetic activity indices had value Apmax = 179 (on November 8, 1998). However, the electron flux only exceeded the dangerous level of 500 particles·cm^{-2}·s^{-1}·sr^{-1} for 1.5 days. The solar source of the event under consideration was a coronal mass ejection (with an initial velocity of 1118 km/s) associated with the M8.4 flare (N22W18) on November 5 at 19:00 UT.

TYPICAL EXAMPLES OF ELECTRONIC ENHANCEMENTS WITH FLUENCE >10^9 particles·cm^{-2}·sr^{-1}·d^{-1} FROM DIFFERENT TYPES OF SOLAR SOURCES

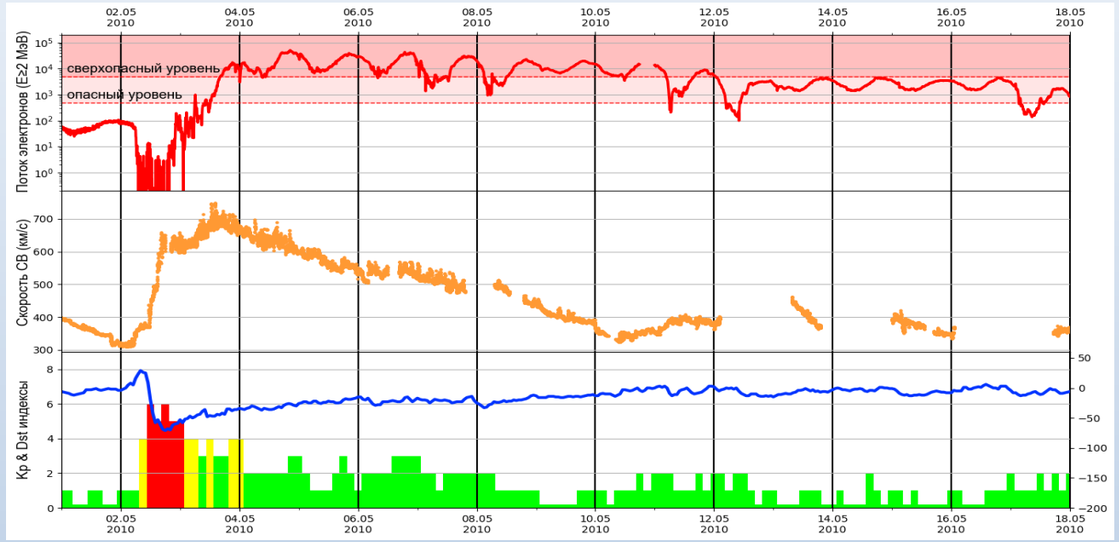

Electron flux with energy >2 MeV, solar wind speed and Kp and Dst indices of geomagnetic activity 1 – 17 May 2010

CH

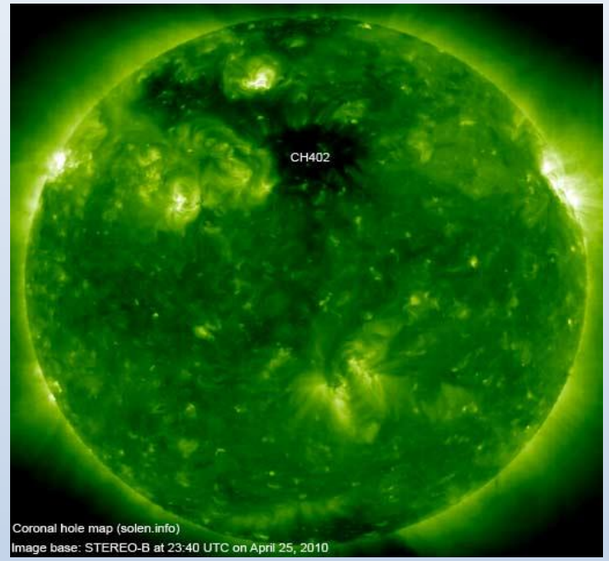

STEREO-B 195 image at 23:40 UTC on April 25

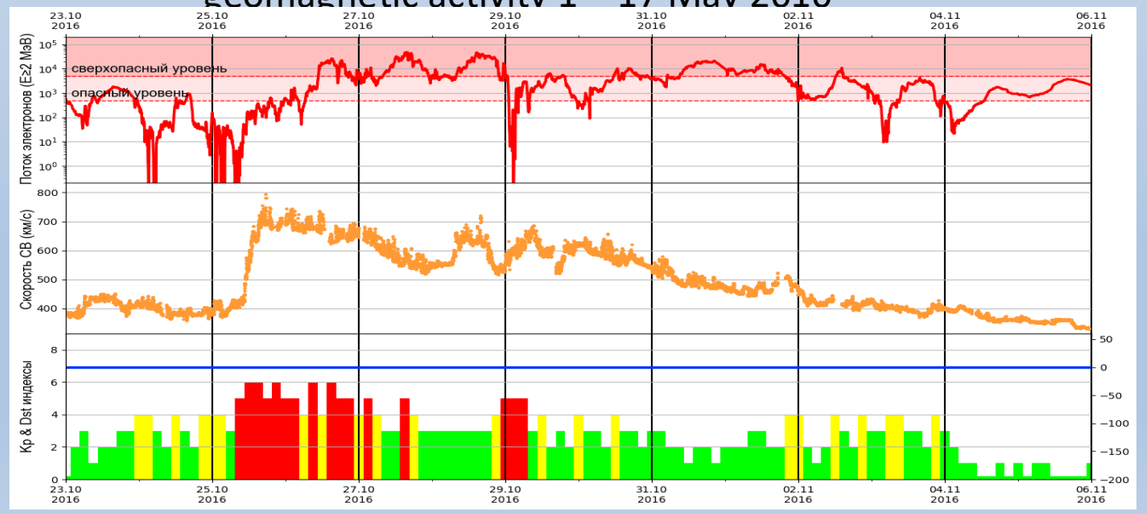

Electron flux with energy >2 MeV, solar wind speed and Kp and Dst indices of geomagnetic activity October 23 – November 3, 2016

CH+DSF

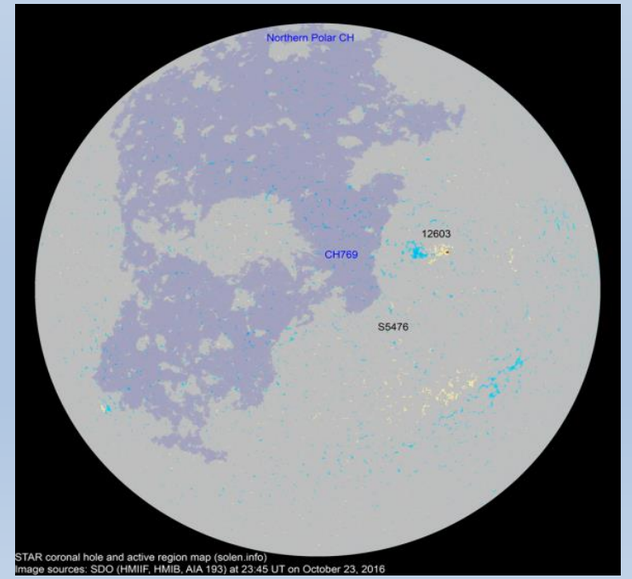

SDO 193 image at 23:45 UTC on October23, 2016

EXAMPLE OF ELECTRONIC ENHANCEMENT WITH FLUENCE >10^8 particles·cm^{-2}·sr^{-1}·d^{-1} OCCURRED AGAINST A QUIET AND UNSETTLED GEOMAGNETIC BACKGROUND

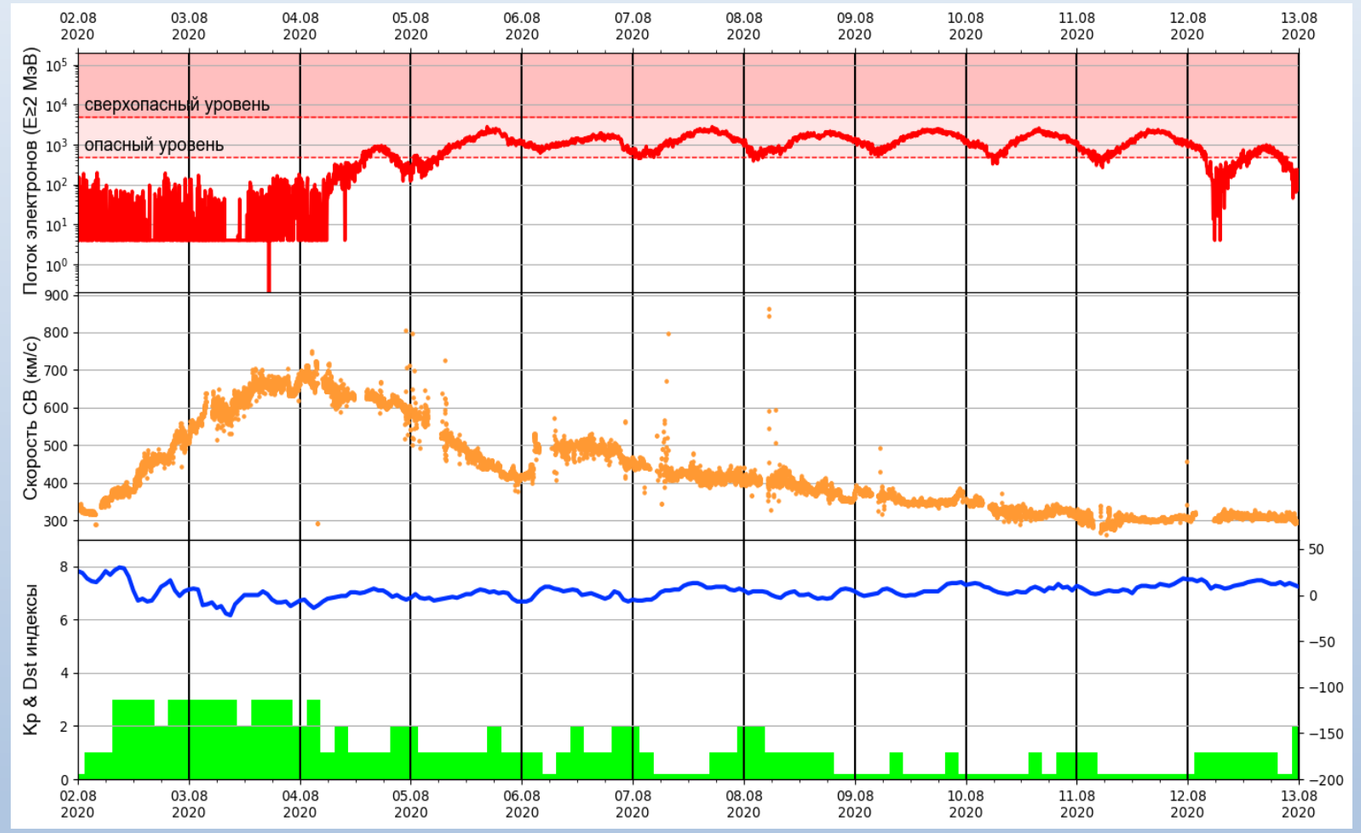

Electron flux with energy >2 MeV, solar wind speed and Kp and Dst indices of geomagnetic activity on 2020 August 2 –12.

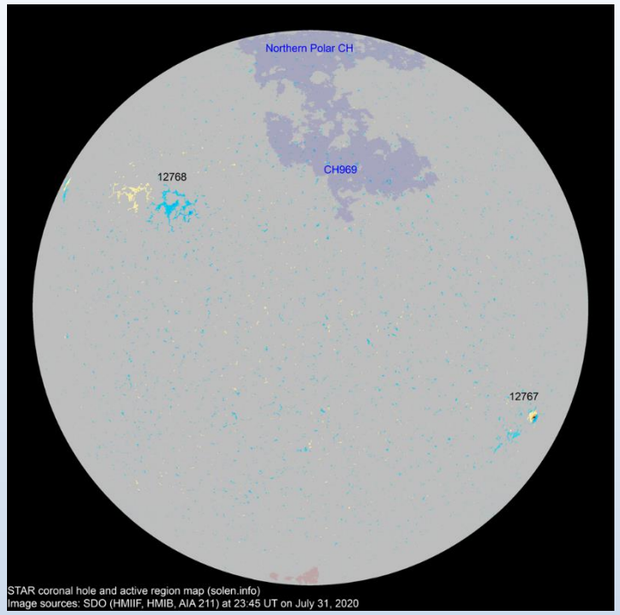

https://solen.info/solar/old_reports/

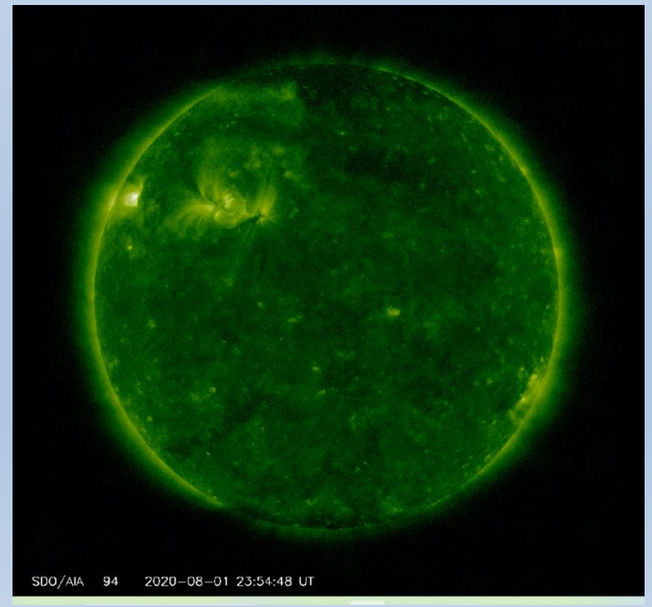

EXTREME ELECTRON FLUX ENHANCEMENT WITH FLUENCE >10^9 particles·cm^{-2}·sr^{-1}·d^{-1} FROM DIFFERENT TYPES OF SOLAR SOURCES

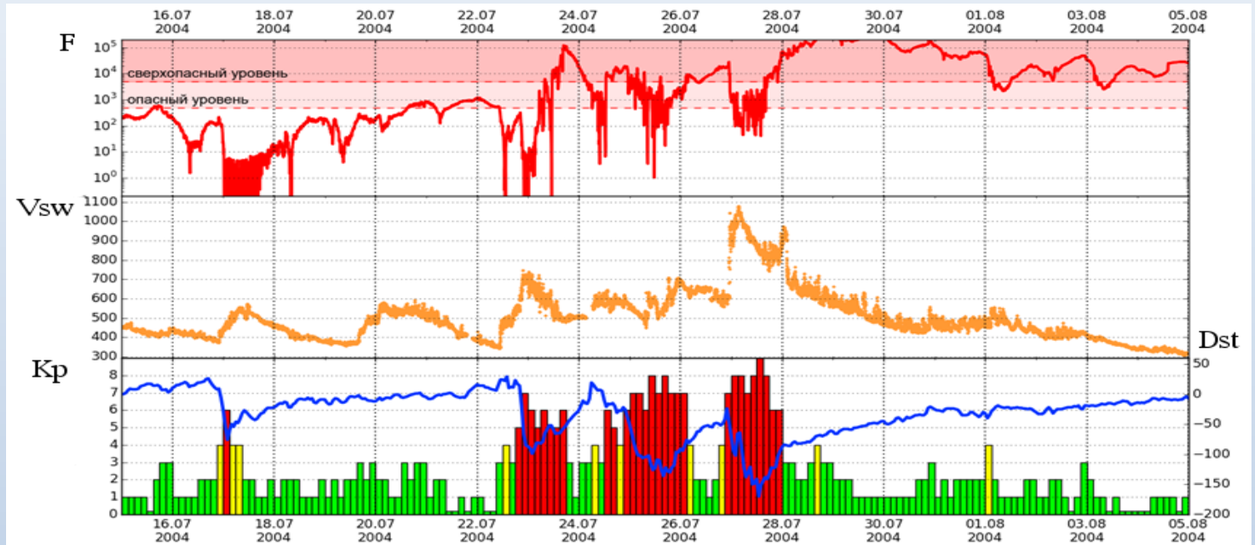

Electron flux with energy >2 MeV, solar wind speed and Kp and Dst indices of geomagnetic activity on July 11-23, 2004.

SF – 22.07
SF+SF+SF -24.07
SF+SF – 26.07
CH+SF – 27.07

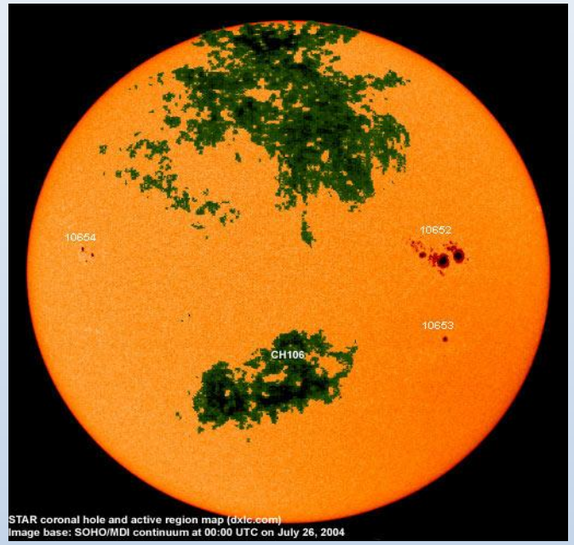

SOHO/MDI image at 00:00 UTC on July 25, 2004

Extreme magnetic storm (Ap = 300, Kp=9-), the maximum fluence for all years of observation (1986-2023) was 9.3 × 10^9 particles·cm^{-2}·sr^{-1}·day^{-1} and was observed on July 29, 2004.

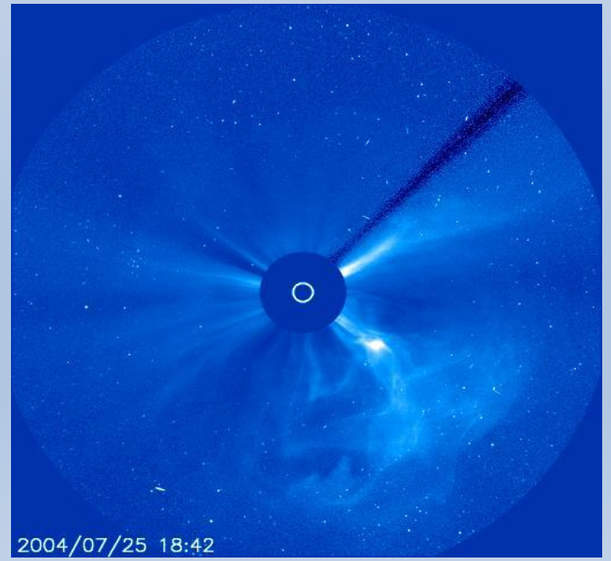

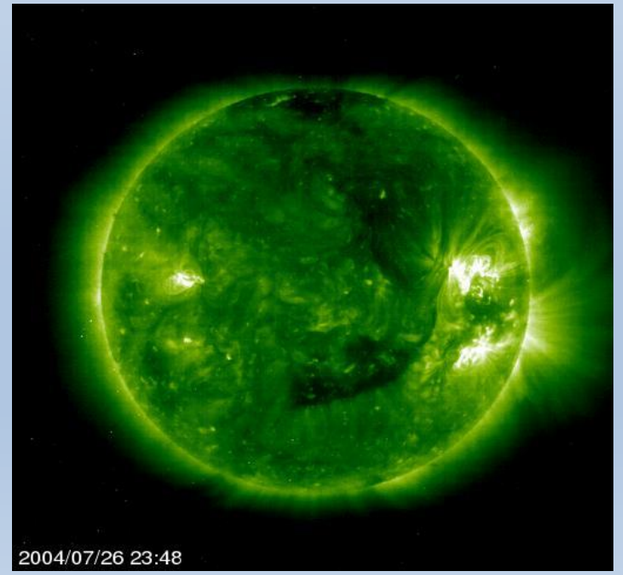

SOHO/EIT 195 image at 23:48 UTC on July 26, 2004

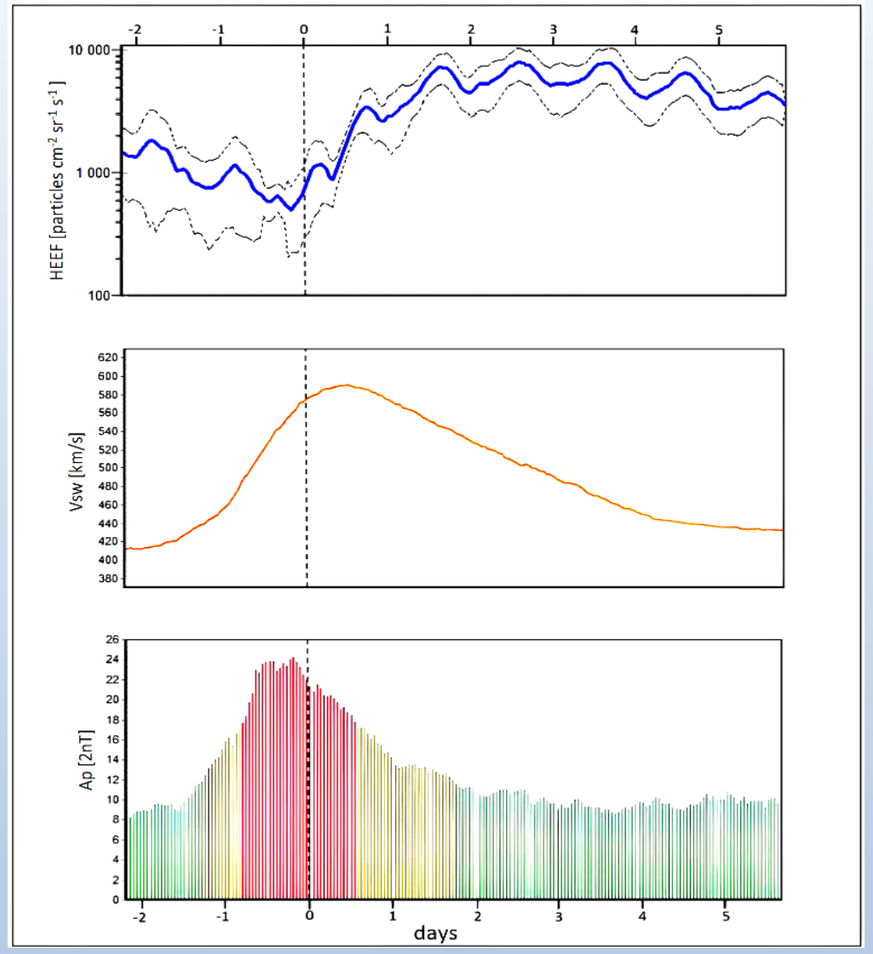

Behavior of the hourly averaged high-energy electron flux, SW velocity and the Ap-index of geomagnetic activity, obtained by epoch superposition method for the high-energy electron flux enhancements after arrival of HSSs from CHs in 1995-2023

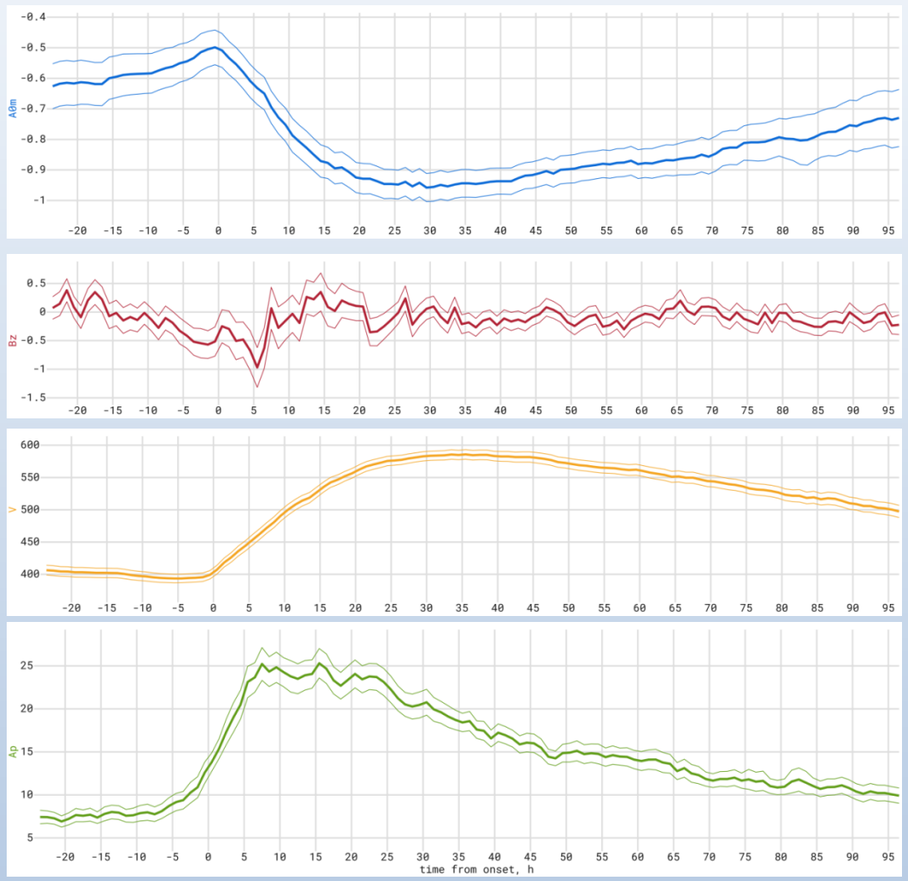

Behavior of the hourly averaged cosmic ray density A0, Bz, SW velocity and the Ap-index of geomagnetic activity, obtained by epoch superposition method for the high-energy electron flux enhancements after arrival of HSSs from CHs in 1995-2023

3. Results

Distribution of the number of electron flux enhancement events depending on the types of their solar sources

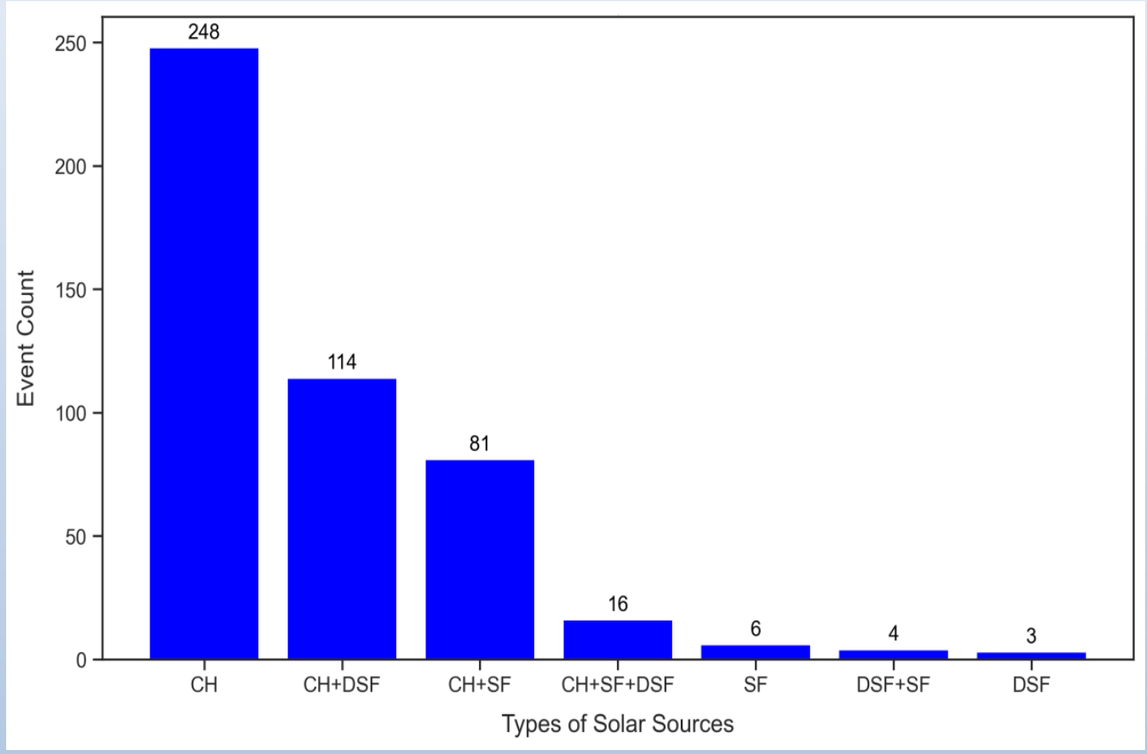

It is evident from the presented distribution that more than half of the high-energy electron flux enhancements (52.5%) are associated with the arrival of HSSs from CHs to the Earth. In addition, in another 44.7% of cases, electron enhancements were preceded by disturbances caused by the combined effect of an HSS from CH and a CME.

Only isolated events (13 HEEF enhancements for the entire studied period 1995-2023, i.e. 2.8%) can be attributed to events caused by interplanetary disturbances, in the formation of which only CMEs participated.

AVERAGE CHARACTERISTICS OF EVENTS CAUSED BY HSSs AND CMEs

Group	V_{max}	B_{max}	$B_{z\,min}$	Dst_{min}	Kp_{max}	Ap_{max}
CH	642.5±5.1	12.78±0.26	-6.28±0.18	-43.47±1.23	4.86±0.06	48.63±1.59
CME	621.5±33.5	23.38±2.77	-13.25±1.72	-101.00±13.60	6.34±0.37	114.3±20.3

Average characteristics of different interplanetary disturbances that caused the HEEF enhancements in 1995-2023 (threshold of electron increases – 10^8 particles·cm^{-2}·sr^{-1}·day^{-1})

The table shows that the IMF increase in the CME group is almost twice as large as in the CH group (based on Bmax and Bz min values). Also, the increase of geomagnetic activity in the CME group is much more significant than in the CH group.

Kryakunova et al. On solar sources of interplanetary disturbances leading to high-energy magnetospheric electron enhancements in geostationary orbit. Monthly Notices of the Royal Astronomical Society, 2025.

3. Results

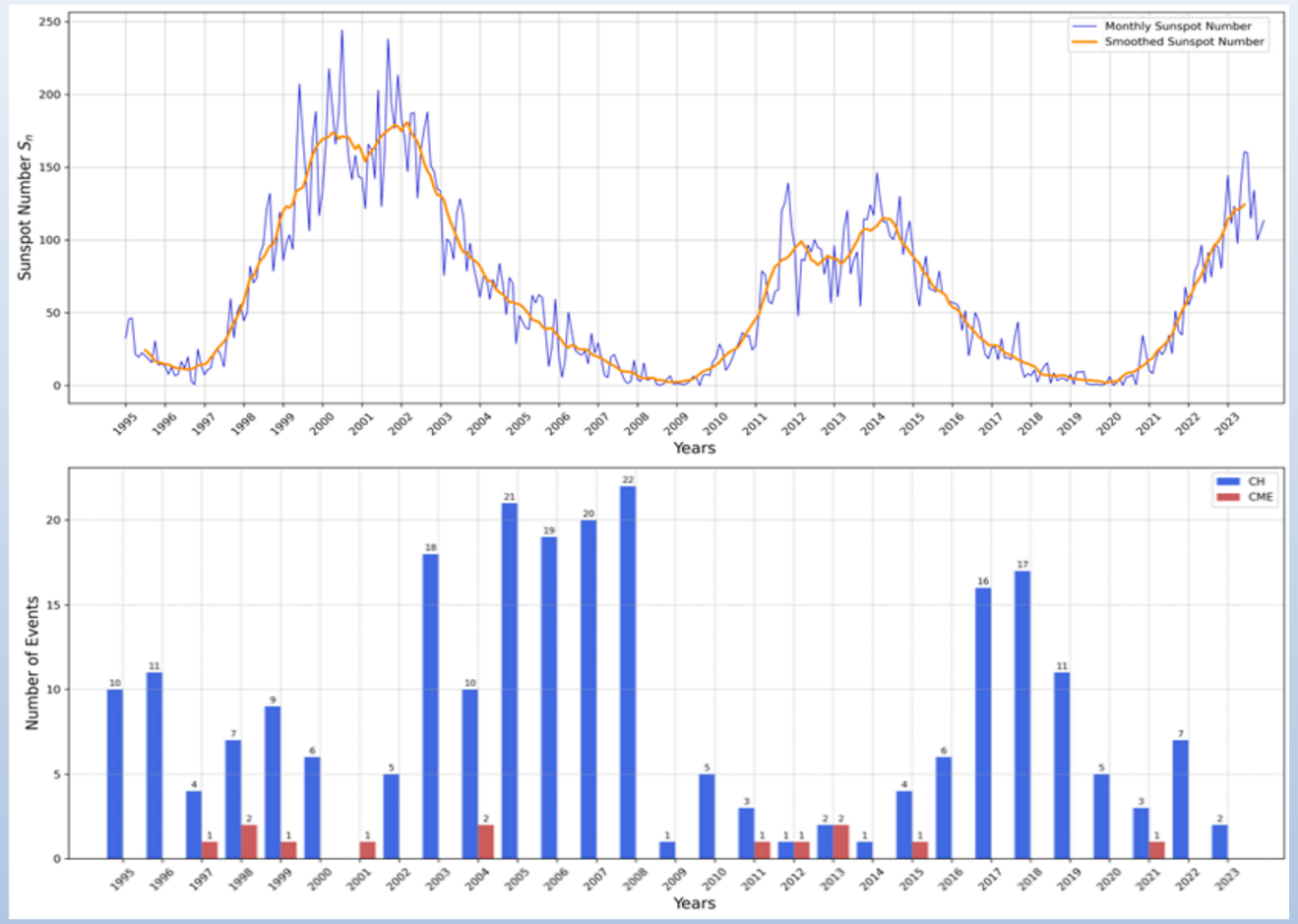

➢High-energy electron flux enhancements following interplanetary disturbances associated with HSSs from CHs occur mainly during the declining phase of the solar cycle and at solar activity minimum, and rare events following interplanetary disturbances associated with CMEs occur near solar activity maxima.

Monthly sunspot numbers with their smoothed values (upper panel) and distribution of high-energy electron flux increases in solar activity cycles depending on its solar sources (blue bars – CH group, red bars – CME group in the lower panel).

Kryakunova et al. On solar sources of interplanetary disturbances leading to high-energy magnetospheric electron enhancements in geostationary orbit. Monthly Notices of the Royal Astronomical Society, 2025.

4. Conclusions

- Solar sources of interplanetary disturbances, after which increases in fluxes of high-energy magnetospheric electrons with energies >2 MeV occur in geostationary orbit, can be both HSSs from CHs and CMEs after SFs and DSFs.
- Of the 478 events of high-energy electron flux enhancements, in 248 events the source of corresponding interplanetary disturbances were only HSSs from CHs, which is 52.5%. In 44.7% of the events the sources were mixed solar events associated with the impact of HSSs from CHs and CMEs after SFs and DSFs.
- On average (epoch superposition method data) enhancements of high-energy electrons in geostationary orbit above the dangerous level (>500 particles·cm^{-2}·s^{-1}·sr^{-1}) due to interplanetary disturbances from HSSs from CHs occur when geomagnetic activity increases to the level of a minor magnetic storm and at a high SW speed (V_{sw}= 590 km/s).
- The IMF strengthening and geomagnetic activity increase in the CME group significantly exceed the corresponding values for the CH group, however, the mean duration of high-energy electron flux increases after HSSs from CHs is 5 days, and due to CMEs influence – 3.5 days. On average, the electron fluence for the CH group reaches 5.4·10^{8} particles·cm^{-2}·sr^{-1}·day^{-1}, and for CMEs – 3.3· 10^{8} particles·cm^{-2}·sr^{-1}·day^{-1}, however, such events occur very rarely, in 2.8% of cases of all discussed high-energy electron flux enhancements.
- High-energy electron flux enhancements following interplanetary disturbances associated with HSSs from CHs occur mainly during the declining phase of the solar cycle and at solar activity minimum, and rare events following interplanetary disturbances associated with CMEs occur near solar activity maxima.

Thank you for your attention !



The "Sun - Man" petroglyph in Tamgaly-Tas near Almaty in Kazakhstan